Hindawi
Mathematical Problems in Engineering
Volume 2017, Article ID 6748160, 13 pages
https://doi.org/10.1155/2017/6748160

Research Article

Research on the Matching of Fastener Stiffness Based on Wheel-Rail Contact Mechanism for Prevention of Rail Corrugation

Caiyou Zhao,[1,2] Ping Wang,[1,2] and Mengting Xing[1,2]

[1] *Key Laboratory of High-Speed Railway Engineering, Ministry of Education, Southwest Jiaotong University, Chengdu 610031, China*
[2] *School of Civil Engineering, Southwest Jiaotong University, Chengdu 610031, China*

Correspondence should be addressed to Ping Wang; 381657901@qq.com

Received 24 October 2016; Revised 9 January 2017; Accepted 15 January 2017; Published 29 March 2017

Academic Editor: Mohammed Nouari

Laying shock absorber fasteners is one of the effective countermeasures used to reduce the ground vibration induced from urban rail transit. However, this kind of fasteners could cause severe rail corrugation. Based on the "wheel-rail dynamic flexibility difference" mechanism, the optimization and further research of fastener stiffness were performed. With the finite element method, the simple beam and board model of the rail system is established to study the vertical and lateral dynamic flexibility characteristics of rails below 1,200 Hz. Within 5–40 kN/mm, a comparison is made between wheel-rail dynamic flexibility differences corresponding to the vertical stiffness and lateral stiffness of different fasteners. The results show that 20 kN/mm and 10 kN/mm are the least and most suitable vertical stiffness values of fasteners, respectively; 40 kN/mm and 5–10 kN/mm are, respectively, the least and most suitable lateral stiffness values of fasteners. The research and analysis results can be adopted as references for deciding the fastener stiffness of urban track.

1. Introduction

Urban rail transit provides extremely convenient transportation. At the same time, the environmental impact of vibration and noise has caused extensive concern in society [1, 2]. In order to reduce vibration and noise during the operation of urban rail transit, different types of vibration reduction measures have been taken for rail transit currently in operation. Among them, the laying of shock absorber fasteners in track structures is one of the commonly used vibration reduction measures. However, after a variety of shock absorber fasteners are used, Beijing Subway [3], Shanghai Metro [4], Guangzhou Metro [5], and other vibration damping tracks have different degrees of rail corrugation. Figure 1 shows the rail corrugation in track structures of shock absorber fastener. Rail corrugation refers to a kind of periodic and uneven rail tread defect on the vertical surface of the rail after the new rail is put into use [6]. It not only increases the interaction force between wheel and track and worsens the relationship between wheel and track, but also causes strong vibration of vehicle track structures, lowers the operating stability, is a serious threat to safety, causes noise pollution, and influences people's living standard and quality [7].

It is well known that many factors affect the emergence and development of rail corrugation; different corrugation has different mechanisms, and it is difficult to use one method to completely cure rail corrugation [8–11]. Through research on corrugation and production mechanisms, Grassie and Kalousek [12–14] introduced the fixed wavelength mechanism and damage mechanism and divided corrugation into six types: track noise or pinned-pinned resonance corrugation; corrugation of heavy-duty rail; corrugation of light rail; rutting-type corrugation; other corrugation caused by P2 force resonance; and corrugation of special structural form of track. Meanwhile, through research, experts at home and abroad put forward corresponding control measures, including rail grinding, use of hard rail, control of friction on top of the track, reduction of rail pad rigidity, and use of damping vibration absorber for rail. The rail grinding [15] allows the optimal contact of wheel and track, so as to

Figure 1: Rail corrugation on the track of shock absorber fastener.

reduce the vibration of the wheel set and make the force between wheel and track uniform. It is one of the most effective measures to relieve corrugation. But the grinding of rail can only remove mild rail corrugation, and the cost of maintenance is high. The train operation density in China is high, the "skylight" time is short, and there is serious lack of efficient grinding equipment. The rigid rail [16] has higher hardness and shear yield strength, so as to have better wear-resisting performance, reduce the sensitivity of rail to the high contact stress, and control rail corrugation. But the production technology of steel is limited; it is difficult to substantially improve the quality of rail, and the cost is restrictive. Control of friction on top of the track [17] can reduce surface friction and corresponding energy loss, thus helping to improve the wear and fatigue resistance of rail and effectively controlling abrasion. Liquid lubricant and other solutions usually adopted can reduce the friction coefficient, but there is the risk of accelerating the development of fatigue crack. By reducing the stiffness of rail pad [18], we can reduce the probability of stick-slip vibration of wheel set, which helps to reduce the additional dynamic action of wheel and track and delay the formation and development of rail corrugation. But the rail pad is made of viscoelastic high polymer material, the stiffness characteristic is not stable, the operation is difficult, and there is the risk of abnormal corrugation. By using the damping vibration absorber of rail [19], we can reduce the self-excited friction vibration of wheel and track, restrain, and reduce the corrugation of the wheel and track system. However, the installation is limited, and weather resistance and maintainability are poor, which may affect the stability of the track.

The fixed wavelength mechanism is obtained from the dynamic interaction between wheel set and track. The damage mechanism is obtained from plastic deformation, rolling contact fatigue, and wear. Most of these theoretical and experimental researches are around wheel and track contact, train structure, track structure, and other aspects. However, another key factor influencing the rail corrugation is the relationship between change of discontinuous support stiffness of the track system and the dynamic flexibility of wheel and track [20] has not been studied in depth. The influence law has not been known clearly. In 2014, through simulation and experimental research, Wang et al. [21] put forward the mechanism of wheel-rail dynamic flexibility difference for the first time, which can effectively describe the cause of short-pitch (25–80 mm) corrugation of the rail. Through experimental verification and comparison and analysis of the actual corrugation of rail under the conditions of different lines and operating conditions, the consistent conclusion was reached. In urban rail transit, the train running speed is low; short-pitch corrugation mainly results with wavelengths of 25–80 mm. No effective control measure has been found yet. According to the new corrugation mechanism of rail, the reduction of wheel-rail dynamic flexibility difference can effectively inhibit the formation and development of rail corrugation. Fastener stiffness is one of the important parameters of track structures and the main design parameter of shock absorber fastener performance. Fastener stiffness has a great impact on the characteristics of abnormal rail corrugation [22–24]. Therefore, based on the mechanism of the wheel-rail dynamic flexibility difference, through the vibration level of rail itself in vertical and horizontal direction, this paper studies the optimal selection of fastener stiffness.

2. The Mechanism of Wheel-Rail Dynamic Flexibility Difference

The formation and development process of rail corrugation is the cyclic process of the interaction between dynamic behaviour of vehicle track and corrugation. When a vehicle passes an irregular track, vibration occurs between the vehicle and track, resulting in uneven wear and plastic deformation of the wheel-rail contact surface; when another vehicle passes, the irregular track and the accumulated uneven wear and plastic deformation of rail contact surface in turn increase the vibration of vehicle and track and result in corrugation on the rail contact surface after repeated cycles [12].

Due to the discontinuous support characteristic of the rail system, changes occur in the dynamic flexibility of rail in the direction of the track. Especially at the pinned-pinned frequency, the dynamic flexibility of the rail above the fastener is quite different from that in the mid-span position. The instability of the track itself is greatly increased. When the wheels roll along the rail, the wheel-rail dynamic flexibility varies by the positions of the actions points, forming the wheel-rail dynamic flexibility difference. This means under the action of the same exciting force, the vibration

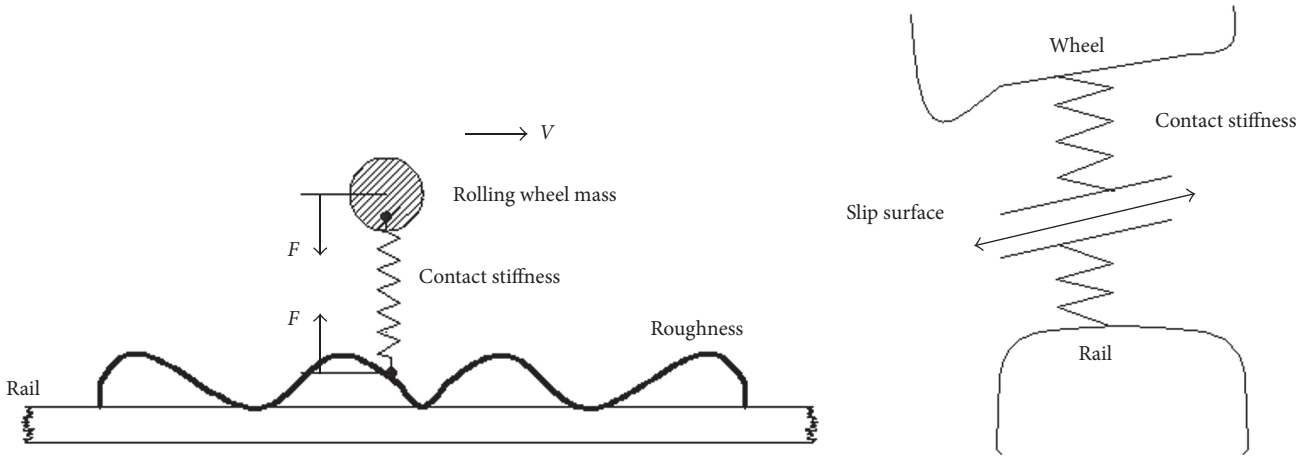

(a) Vertical-longitudinal model (b) Vertical-lateral model

Figure 2: Interaction of wheel-rail rolling.

displacement of the rail is different from that of the wheel. In the process of wheel-rail contact, such vibration displacement difference will lead to the change and cyclical fluctuation of wheel-rail contact force. The larger the wheel-rail dynamic flexibility difference, the bigger the cyclical fluctuation and the more serious the corrugation is [21].

The new rail corrugation mechanism, "wheel-rail dynamic flexibility difference" mechanism, proposed by studying the relationship between the change of support stiffness of the rail system and the dynamic flexibility of the wheel-rail system mainly has two aspects: (1) the impact effect in the vertical direction and (2) The sliding wear effect in the lateral direction. In urban rail transit lines, the train running speed is relatively low. The frequency corresponding to the short-pitch (25–80 mm) corrugation is mainly below 800 Hz, which is near the lateral pinned-pinned frequency of the rail. It can effectively describe the cause of short-pitch (25–80 mm) corrugation of the rail [25]. By reducing the wheel-rail dynamic flexibility difference and controlling the vibration of rail, we can effectively inhibit the formation and development of short-pitch corrugation of rail.

2.1. The Impact Effect in the Vertical Direction. Because when rolling along the rail wheels have different positions of action point and the wheel-rail dynamic flexibility difference exists, an unsteady dynamic force is produced on the wheel-rail contact surface mainly in the vertical direction, as shown in Figure 2(a). Under the action of unsteady dynamic vertical wheel-rail exciting force, at the frequency higher than a specific frequency (such as pinned-pinned frequency), the vibration displacement of the rail is greater than the vibration displacement of the wheels, so that the unsteady rolling of "contact-separation-collision-contact" occurs between the rails and wheels. If the wheel-rail dynamic flexibility difference is very large at a certain frequency, with the constant track condition and speed, the change of wheel-rail contact force forms the cyclical fluctuation due to the "contact-separation-collision-contact," so that the change trace with fixed pitches is formed on the wheel-rail contact surface when the wheels roll along the rail. And it can be considered qualitatively that the rail corrugation becomes severe with the increasing of the wheel-rail dynamic flexibility difference.

2.2. The Sliding Wear Effect in the Lateral Direction. When wheels roll along the rail, due to the slope design of wheel-rail contact surface, there is lateral sliding on the contact surface in addition to the longitudinal rolling and longitudinal sliding along the track. Laterally, there exists difference between the wheel and track in dynamic flexibility, especially in the p-p frequency section and longitudinal dynamic flexibility along the rail. Due to the lateral periodic relative vibration displacement difference, sliding friction and wear occur on the wheel-rail contact surface. When the vehicle speed is constant, the component of lateral vibration and vertical vibration of the rail leads to contact force fluctuation and lateral alternating sliding, as shown in Figure 2(b). Due to the longitudinal change of wheel-rail dynamic flexibility difference along the rail and the longitudinal change of wheel-rail contact force, wear on the surface of the rail shows standing wave-type scratches in the longitudinal direction.

3. Modelling and Theoretical Calculation

3.1. Modelling. The actual rail system is a structure with infinite length, but computer ability is limited and the calculation model cannot be expanded endlessly. Therefore, a section of the track system is cut for the finite element analysis of the infinitely long rail system. To eliminate the boundary effect and consider the calculation speed, in this paper the model length is a spacing of 131 fasteners. Among them, the fastener spacing is 0.625 m, which means the model is 81.875 m long.

The track structure adopted in the urban rail traffic in China is simplified; a simple beam and board model of the track system is established, as shown in Figure 3. It mainly includes rail, fasteners and the monolithic track bed. The rail is equivalent to the infinitely long point-supporting beam, and BEAM18 unit is used for simulation; fasteners

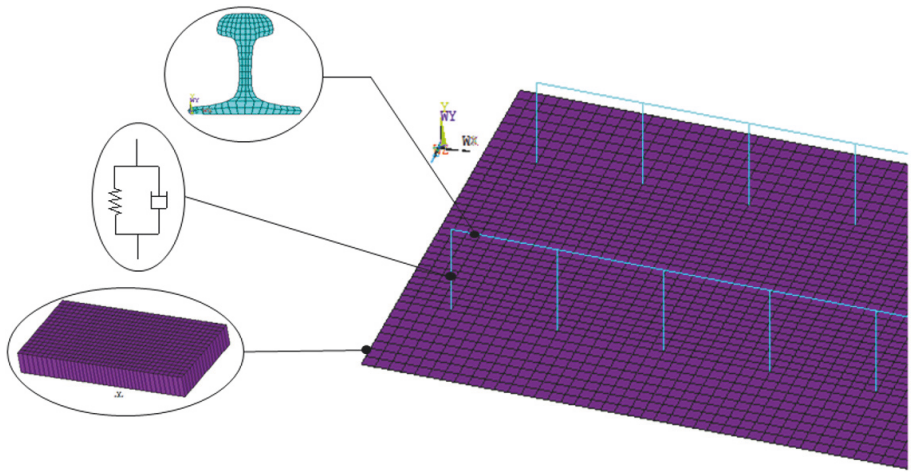

Figure 3: Simple beam and slab model of the track system.

are equivalent to elastic elements, the vertical and lateral direction is equivalent to linear springs, and COMBIN14 unit is used for simulation; the monolithic track bed is considered as the length of the model (81.875 m) and equivalent to the shell, and SHELL63 unit is used for simulation. Fixed constraints are adopted on both ends of the rail. For the monolithic track bed, according to actual conditions, the longitudinal, lateral, and vertical displacements are constrained.

3.2. Theoretical Derivation of the Dynamic Flexibility. Dynamic flexibility is the vibration response under the action of unit force and one of the transmission response functions. In this paper, it is used to reflect the vibration characteristics and transfer rules of the track structure.

The dynamic equilibrium equation of the track system is described with the following formula:

$$C\frac{du(t)}{dt} + Ku(t) = -M\frac{du(t)^2}{dt^2} + F(t), \tag{1}$$

where $u(t)$ is the vibration displacement of the rail at time t, C is damp of the fastener system, K is stiffness of the fastener system, and $F(t)$ is the exciting force acting on the rail.

Assume that vibration displacement is

$$u(t) = A_x e^{-i\omega t}. \tag{2}$$

Then

$$u(t)\left(-i\omega C + K - \omega^2 M\right) = F(t). \tag{3}$$

Therefore, dynamic flexibility can be expressed as follows:

$$\partial = \frac{u(t)}{F(t)} = \frac{1}{-i\omega C + K - \omega^2 M}. \tag{4}$$

Dynamic flexibility ∂ consists of amplitude $\partial(\omega)$ and phase $\varphi(\omega)$.

$$\begin{aligned} \partial(\omega) &= \frac{1}{K}\sqrt{\frac{1}{\left(1-\omega^2/\omega_e\right)^2 + \left(4\xi^2\left(\omega^2/\omega_e{}^2\right)\right)^2}} \\ \varphi(\omega) &= \tan^{-1}\left\{\frac{2\xi}{\left(\omega/\omega_e - \omega_e/\omega_e\right)}\right\}, \end{aligned} \tag{5}$$

where ω is the angular frequency and $\omega = 2\pi f$; ω_e is the eigenfrequency and $\omega_e = \sqrt{K/M}$; ξ is the attenuation rate and $\xi = C/2\sqrt{KM}$.

4. Dynamic Flexibility Characteristics of the Rail

4.1. Calculation of Dynamic Flexibility of the Rail. Based on the beam and board model established in this paper, with two adjacent fasteners in the middle of the model as the research object, the unit resonant force is applied on the rail, and the harmonic response analysis is conducted. The dynamic flexibility at the frequency of 0~1,200 Hz [26] on different positions along the longitudinal beam of rail in the vertical and lateral direction can be calculated. The model parameters are shown in Table 1.

There are two kinds of working conditions above the rail fasteners and on the cross section 1/2 of the fastener span, the unit resonant force is applied, respectively, in the vertical and lateral directions, and vertical and lateral dynamic flexibility spectrum of the rail is obtained, as shown in Figures 4(a) and 4(b), respectively.

The first peak shown in Figure 4 is the rail resonance. The vertical resonance frequency is 170 Hz, and the lateral resonance frequency is 80 Hz. The corresponding vibration mode is as shown in Figures 5(a) and 5(b), respectively. The second peak depicted in Figure 4 is the first-order pinned-pinned resonance. The vertical and lateral frequencies are 1,020 Hz and 440 Hz, respectively. The standing wave node is just above the fastener, and the wavelength is the spacing

Table 1: Main parameters of beam and board model of the track structure.

Part	Item	Unit	Value
Rail	Section	kg/m	60
	Elasticity modulus	MPa	2.06×10^5
	Poisson's ratio	—	0.3
Fastener	Vertical stiffness	kN·mm^{-1}	40
	Vertical damp	kN·s·m^{-1}	10
	Lateral stiffness	kN·mm^{-1}	10
	Lateral damp	kN·s·m^{-1}	10
	Fastener spacing	m	0.625
Track bed slab	Elasticity modulus	MPa	3.35×10^4
	Poisson's ratio	—	0.2
	Thickness	m	0.26

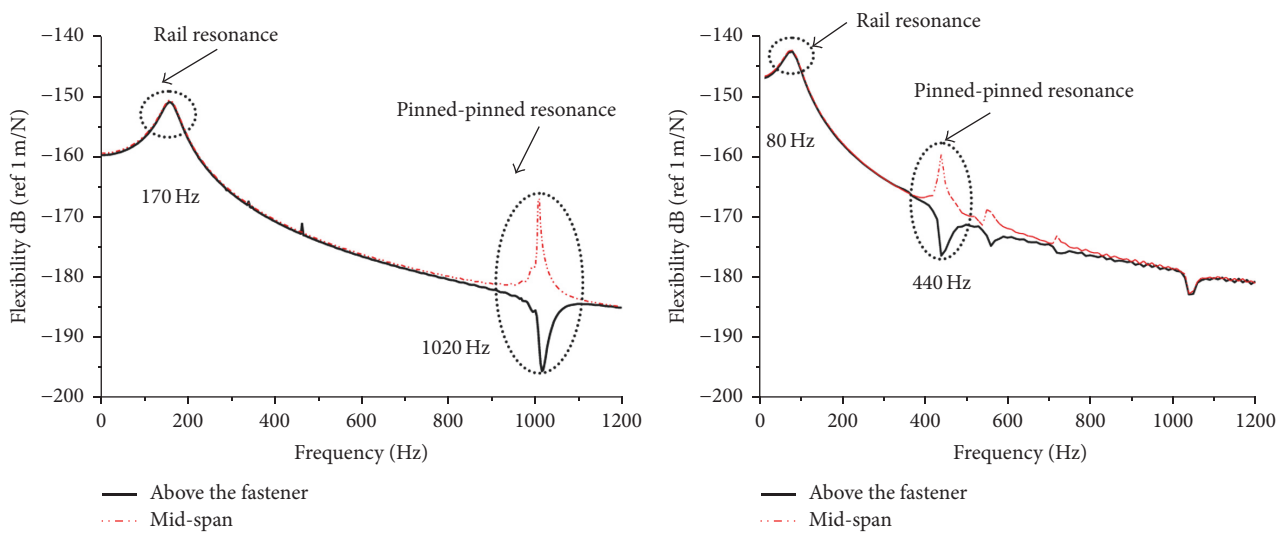

(a) Vertical dynamic flexibility spectrum

(b) Lateral dynamic flexibility spectrum

Figure 4: Rail dynamic flexibility spectrums.

between two fasteners (1.25 m in this paper), as shown in Figures 6(a) and 6(b). Due to discontinuous bearing of the rail, the dynamic flexibility of rail above the fastener and on the mid-span section varies considerably.

4.2. Change of Longitudinal Dynamic Flexibility of the Rail. In order to further study the vertical and lateral dynamic flexibility change on different positions on the longitudinal beam of the rail, with adjacent four fasteners in the middle of the model as the research object, the coordinate system is established, as shown in Figure 7.

Half of the fastener spacing is a cycle. Each cycle is equally divided to select loading points. There are a total of nine different loading positions, as shown in Figure 6. At the vertical pinned-pinned frequency of 1,020 Hz and lateral pinned-pinned frequency of 440 Hz of the rail, the curve of dynamic flexibility on different positions along the longitudinal beam is as shown in Figures 8(a) and 8(b), respectively.

Figure 8 shows that when the rail is at pinned-pinned frequency, the dynamic flexibility on different positions of the rail increases at first and decreases later above the fastener in mid-span above the fastener. The change is cyclical. The change of vertical dynamic flexibility is more than 20 dB, and the change of lateral dynamic flexibility is more than 15 dB. Such dramatic dynamic flexibility change influences the rail corrugation to a large extent. Figures 9(a) and 9(b) show the vertical and lateral dynamic flexibility characteristic on different positions on the rail at different frequencies, respectively.

5. Wheel-Rail Dynamic Flexibility Differences

5.1. Calculation of Dynamic Flexibility of the Wheel. In general, the wheel-rail contact spring is simply considered to only relate to the displacement of wheel and track. However, the wheel-rail dynamic flexibility differences are only studied in this study, not the displacement of wheel and track. And, therefore, the wheel is considered as a single-mass system without spring. Under the action of unit resonant force, its vibration equation is as follows:

$$M_0 \ddot{z}_\omega = e^{j\omega t}. \tag{6}$$

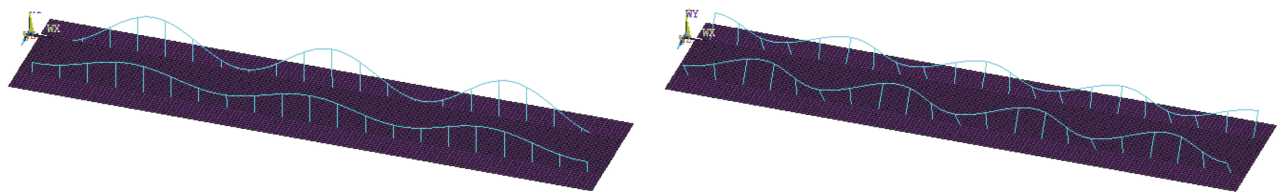

(a) Vertical rail resonance (b) Lateral rail resonance

Figure 5: Vibration mode of rail resonance.

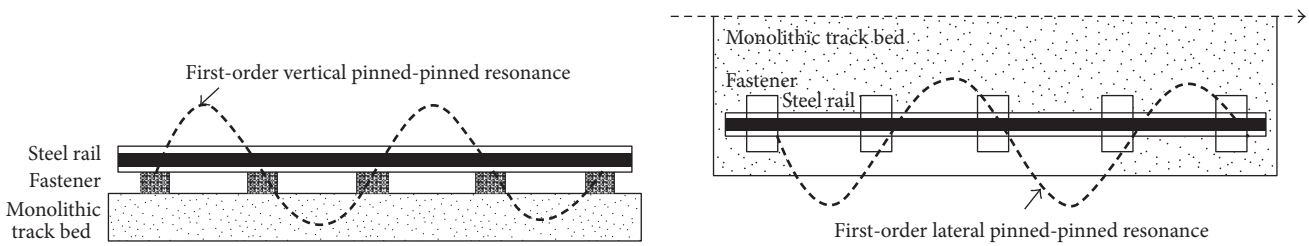

(a) First-order vertical pinned-pinned resonance (b) First-order lateral pinned-pinned resonance

Figure 6: First-order pinned-pinned resonance of the rail.

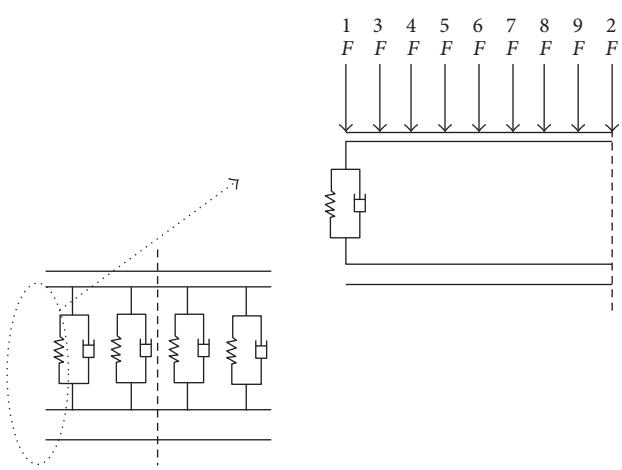

Figure 7: Schematic diagram of loading position of unit resonant force.

Based on the definition of dynamic flexibility of the wheel:

$$z_\omega = \alpha_\omega e^{j\omega t}. \tag{7}$$

Then:

$$\alpha_\omega = -\frac{1}{M_0\omega^2}, \quad \omega = 2\pi f. \tag{8}$$

Assume that the nonsuspension equivalent mass of the vehicle is 800 kg, typical of most vehicles. The vertical and lateral dynamic flexibility spectrum of wheel is shown in Figure 10.

5.2. Wheel-Rail Dynamic Flexibility Difference. Figures 11(a) and 11(b) show the vertical and lateral dynamic flexibility spectrum on the contact points of rail and wheel, respectively, and compare the relative relationship between dynamic flexibility of the wheel and dynamic flexibility of the track vertically and laterally.

Figure 11 shows that within the scope from the rail resonance frequency to the pinned-pinned frequency, the dynamic flexibility of the rail is much higher than dynamic flexibility of the wheel, forming the wheel-rail dynamic flexibility difference. This means that under the same exciting function, the vibration displacement of the rail is greater than the vibration displacement of the wheel. In the process of wheel-rail rolling contact, different vibration displacement characteristics result in the change of wheel-rail contact force and, as a result, cyclical fluctuation occurs. In the urban rail system, due to the existence of the wheel-rail dynamic flexibility difference, the rail has corrugation. Therefore, in order to reduce and control rail corrugation and reduce vibration and noise, we need to reduce the wheel-rail dynamic flexibility difference.

Figures 12(a) and 12(b) show the vertical and lateral dynamic flexibility curve of wheel and track at pinned-pinned frequency on different positions along the rail between half of fastener spacing, respectively. It can be seen that at pinned-pinned frequency, the rail dynamic flexibility changes; the dynamic flexibility above fastener and dynamic flexibility in mid-span are especially quite different, which has great influence on the track structure and rail corrugation generation.

In addition, the wheel-rail dynamic flexibility difference is the difference between dynamic flexibility of the wheel and dynamic flexibility of the rail. The curve of vertical and lateral wheel-rail dynamic flexibility difference with half of fastener spacing on different positions along the rail at pinned-pinned frequency is shown in Figure 13.

As shown in Figure 13(a), the maximum vertical wheel-rail dynamic flexibility difference on different positions along the rail at the pinned-pinned frequency of 1,020 Hz is 2.65 ×

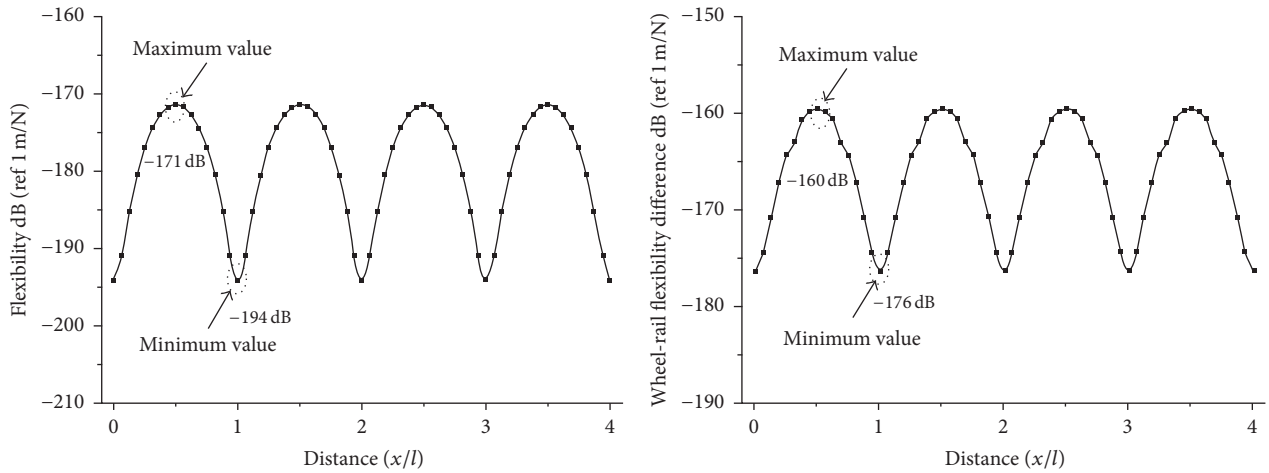

(a) Vertical dynamic flexibility at the pinned-pinned frequency of 1,020 Hz

(b) Lateral dynamic flexibility at the pinned-pinned frequency of 440 Hz

Figure 8: Dynamic flexibility of different positions on the longitudinal beam of rail at pinned-pinned frequency.

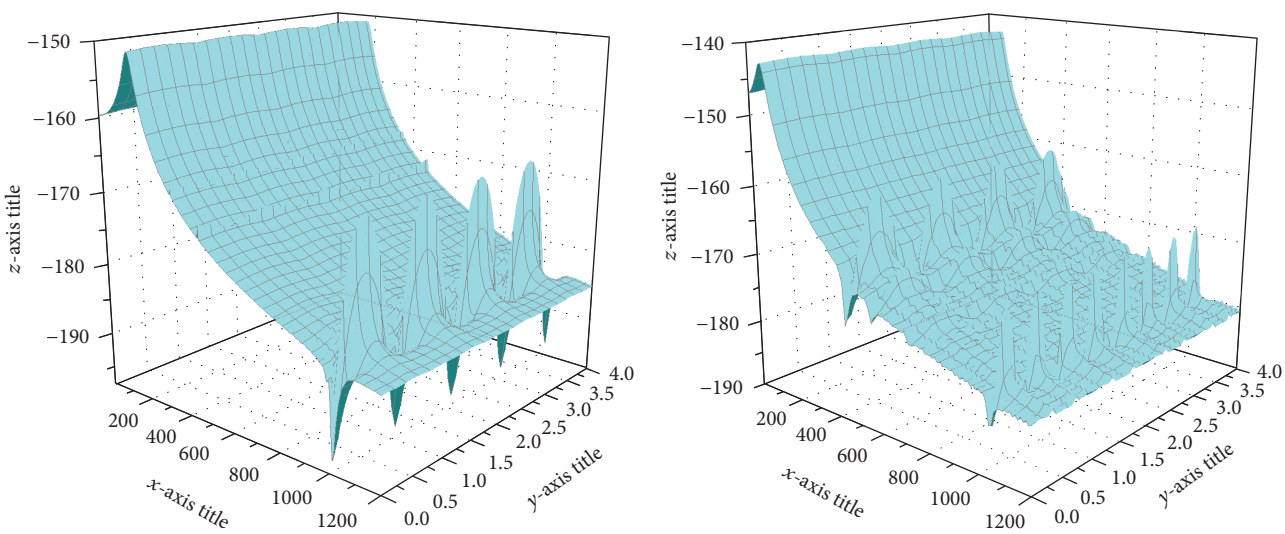

(a) Vertical dynamic flexibility spectrum

(b) Lateral dynamic flexibility spectrum

Figure 9: Dynamic flexibility spectrums on different positions of the rail.

10^{-9} (m/N) appearing in mid-span; and the minimum value is 1.39×10^{-9} (m/N) appearing above the fastener; the difference between them is 1.26×10^{-9} (m/N).

As shown in Figure 13(b), the maximum lateral wheel-rail dynamic flexibility difference on different positions along the rail at the pinned-pinned frequency of 440 Hz is 1.29×10^{-8} (m/N) appearing in mid-span; the minimum value is 9.74×10^{-10} (m/N) appearing above the fastener; the difference between them is 1.1926×10^{-8} (m/N).

At the pinned-pinned frequency, the lateral wheel-rail dynamic flexibility difference is much greater than the vertical wheel-rail dynamic flexibility difference. Short-pitch corrugation mainly appears on the curve track with large radius; this may be associated with the large lateral wheel-rail exciting force.

The wheel-rail dynamic flexibility difference rate is the change rate of wheel-rail dynamic flexibility difference, which controls, to some extent, the speed of formation and development of corrugation. This paper uses the cubic function for the fitting of wheel-rail dynamic flexibility difference curve. By solving the slope of fitting function, the wheel-rail dynamic flexibility difference rate on each position is obtained.

The fitting function of vertical wheel-rail dynamic flexibility difference curve is as follows:

$$y = \left(-4x^3 + 3x^2 - 0.07x + 0.01\right) \times 10^{-8}. \quad (9)$$

The fitting function of lateral wheel-rail dynamic flexibility difference curve is as follows:

$$y = \left(-2x^3 + 2x^2 - 0.03x + 0.01\right) \times 10^{-7}. \quad (10)$$

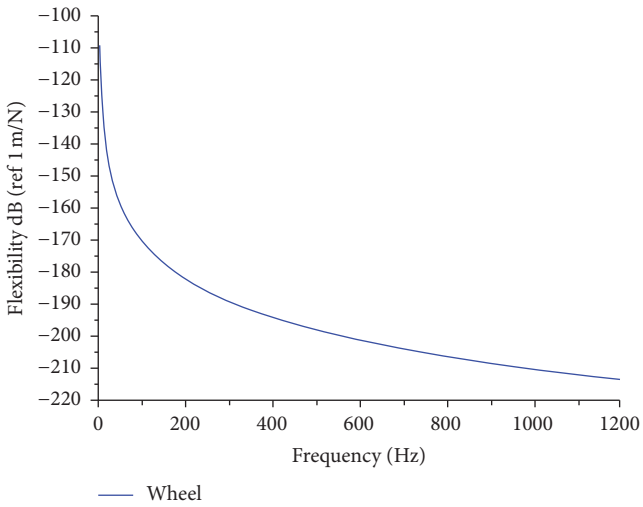

Figure 10: Wheel dynamic flexibility spectrum.

In these, y represents the wheel-rail dynamic flexibility difference and x represents different positions along the rail within half of fastener spacing.

The slope of Formula (9) is the vertical wheel-rail dynamic flexibility difference rate.

$$\dot{y} = \left(-12x^2 + 6x - 0.07\right) \times 10^{-8}. \tag{11}$$

The slope of Formula (10) is the lateral wheel-rail dynamic flexibility difference rate.

$$\dot{y} = \left(-6x^2 + 4x - 0.03\right) \times 10^{-7}. \tag{12}$$

In these, $\dot{y}$ represents the wheel-rail dynamic flexibility difference rate and x represents different positions along the rail within half of fastener spacing.

Therefore, the vertical and lateral wheel-rail dynamic flexibility difference rate curve on different positions along the rail within half of fastener spacing at the pinned-pinned frequency is as shown in Figures 14(a) and 14(b), respectively.

6. Optimal Selection of Fastener Stiffness

According to the "wheel-rail dynamic flexibility difference" mechanism and the formation and development mechanism of rail corrugation, in order to reduce and control the vibration noise at the source, research on the optimal selection of parameters for the urban rail system is crucial based on the principle of lowering the wheel-rail dynamic flexibility difference. In this paper, the optimal selection is mainly implemented for the fastener stiffness.

Fastener stiffness in the urban rail structure is usually 5–40 kN/mm [27]. Vertical stiffness and lateral stiffness of fasteners are adjusted, respectively (Tables 2 and 3), the other parameters of the model remain the same, the unit resonant force is applied on the rail, and the influence law of fastener stiffness is discussed, as to find the most reasonable fastener stiffness.

6.1. Selection of Vertical Stiffness of the Fastener. Under five kinds of working conditions shown in Table 2, the change rule of wheel-rail dynamic flexibility difference is as shown in Figure 15(a). To compare and analyse the wheel-rail dynamic flexibility difference with different vertical stiffness of fastener, the characteristic values include maximum, minimum, and average, as shown in Figure 15(b).

From Figure 15(b), we can know that when the vertical stiffness of fastener decreases from 20 kN/mm to 10 kN/mm or increases to 25 kN/mm, the wheel-rail dynamic flexibility difference drops. When the vertical stiffness of fastener increases from 25 kN/mm to 40 kN/mm, the wheel-rail dynamic flexibility difference increases; so for the vertical stiffness of fastener, 25 kN/mm is better than 40 kN/mm. When the vertical stiffness of fastener reduces from 10 kN/mm to 5 kN/mm, the wheel-rail dynamic flexibility difference increases slightly. When the fastener is installed and used, the stiffness should not be too low, so the vertical stiffness of fastener should ideally be 10 kN/mm. By comparison of the vertical stiffness of fastener at 10 kN/mm and 25 kN/mm, it is found that the wheel-rail dynamic flexibility difference is slightly smaller when the vertical stiffness is 10 kN/mm. According to the above comparison, Working Condition 3 is most unfavourable, and Working Condition 2 is the best.

In order to further compare different vertical stiffness of fastener, the change rule of the wheel-rail dynamic flexibility difference rate is as shown in Figure 15(c).

Based on the wheel-rail dynamic flexibility difference rate corresponding to different vertical stiffness of fastener in Figure 15(c), when the vertical stiffness of fastener is 20 kN/mm, the wheel-rail dynamic flexibility difference rate is the largest, and the wheel-rail dynamic flexibility rates corresponding to the vertical stiffness of other fasteners are similar. To slow down rail corrugation, the change of wheel-rail dynamic flexibility difference should not be too big. Through comprehensive comparison, it can be concluded that the most unfavourable value of vertical stiffness of the fastener is 20 kN/mm, and the best value of vertical stiffness of fastener is 10 kN/mm.

6.2. Selection of Lateral Stiffness of Fastener. The change rule of wheel-rail dynamic flexibility difference under the five kinds of working conditions shown in Table 3 is as shown in Figure 16(a). To compare and analyse the wheel-rail dynamic flexibility difference with lateral stiffness of different fasteners, its characteristic values include the maximum value, the minimum value, and the average value, as shown in Figure 16(b).

From Figure 16(b) we can know that with the increase of lateral stiffness of fastener, wheel-rail dynamic flexibility difference increases. Among them, when the lateral stiffness of fastener increases from 5 kN/mm to 10 kN/mm, the wheel-rail dynamic flexibility difference shows little change. When the fastener is installed and used, the stiffness should not be too small, so the reasonable value range of the lateral stiffness of fastener is 5–10 kN/mm. According to the above comparison, Working Condition 5 is the most unfavourable, and Working Conditions 1 and 2 are better.

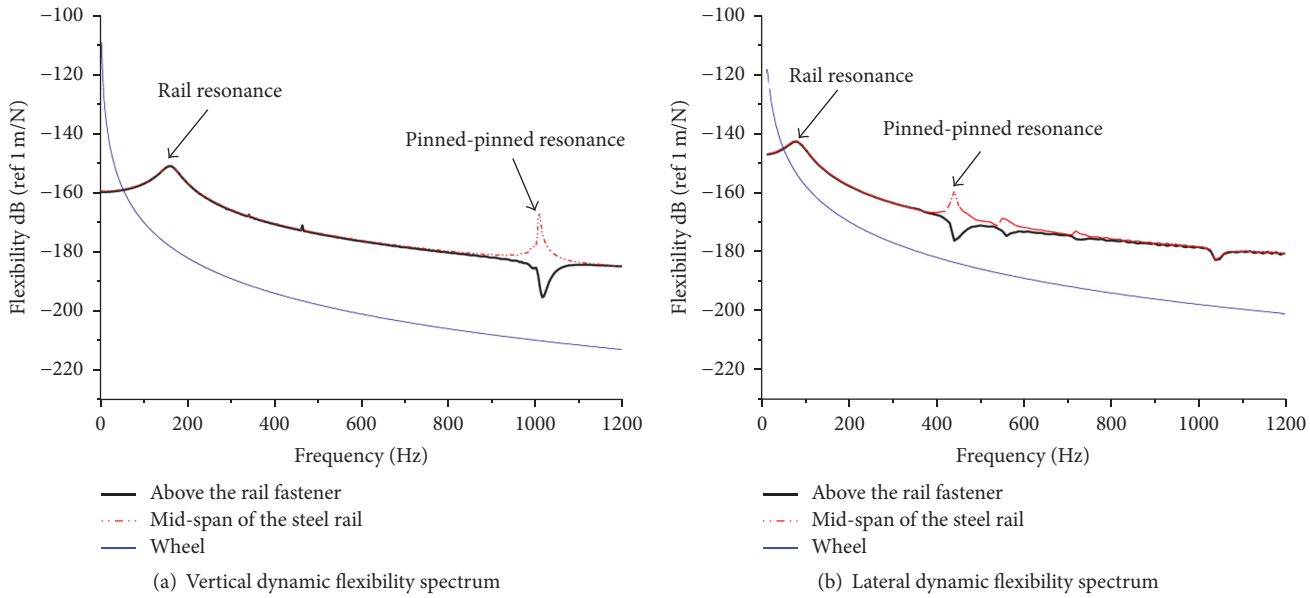

Figure 11: Wheel-rail dynamic flexibility spectrums.

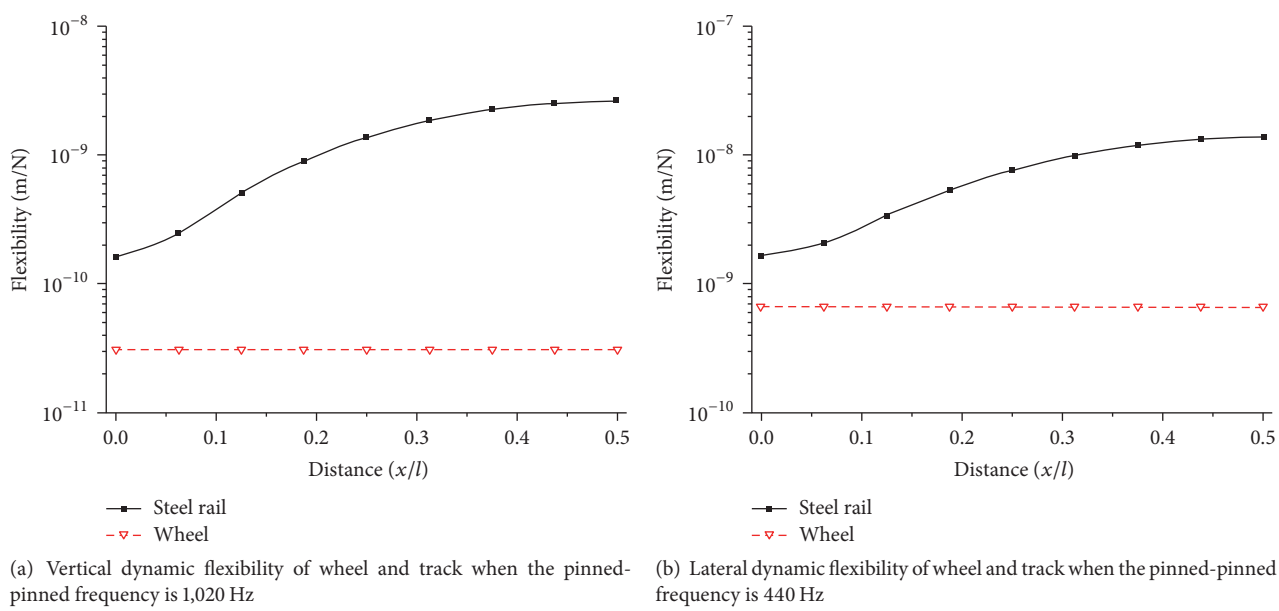

Figure 12: Dynamic flexibility of wheel and track on different positions along the rail at the pinned-pinned frequency.

Table 2: Design of cases for the vertical stiffness of the fastener.

Fastener parameter	Case 1	Case 2	Case 3	Case 4	Case 5
Vertical stiffness/kN·mm^{-1}	5	10	20	25	40
Vertical damp/kN·s·m^{-1}	10	10	10	10	10
Lateral stiffness/kN·mm^{-1}	10	10	10	10	10
Lateral damp/kN·s·m^{-1}	10	10	10	10	10
Fastener spacing/m	0.625	0.625	0.625	0.625	0.625

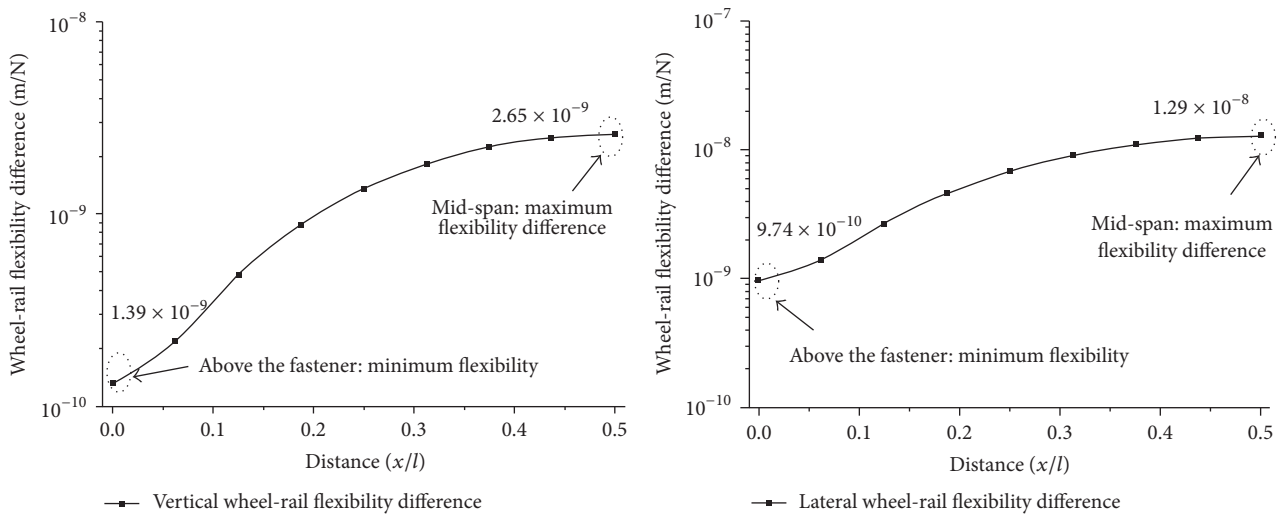

(a) At the pinned-pinned frequency of 1,020 Hz vertical wheel-rail dynamic flexibility difference

(b) At the pinned-pinned frequency of 440 Hz lateral wheel-rail dynamic flexibility difference

Figure 13: The rail wheel-rail dynamic flexibility difference on different positions along the rail at the pinned-pinned frequency.

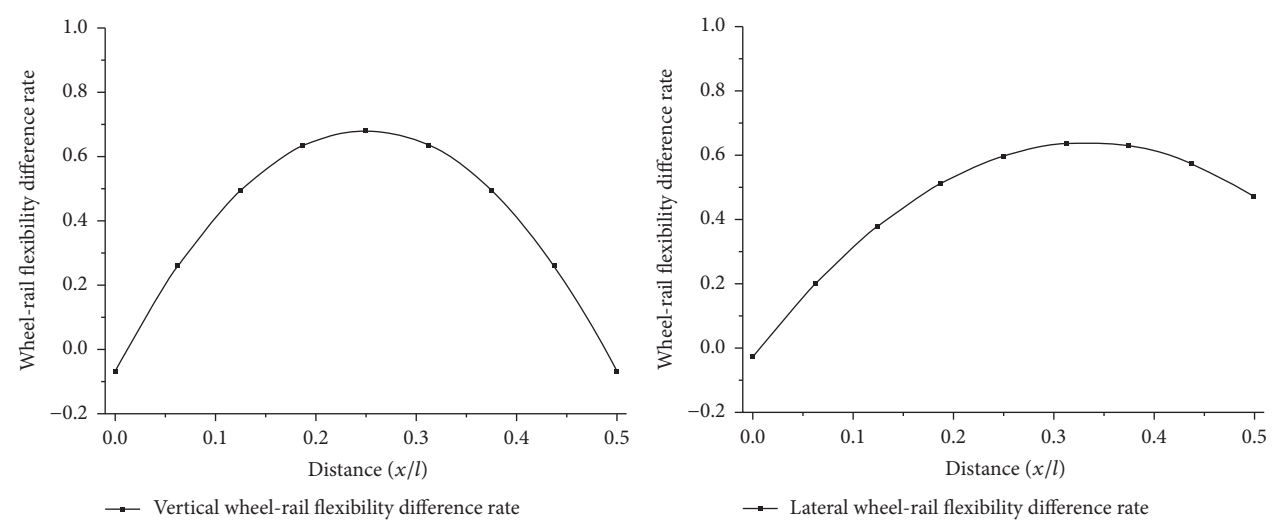

(a) Vertical wheel-rail dynamic flexibility difference rate at the pinned-pinned frequency of 1,020 Hz

(b) Lateral wheel-rail dynamic flexibility difference rate at the pinned-pinned frequency of 440 Hz

Figure 14: Wheel-rail dynamic flexibility difference rates on different positions along the rail at the pinned-pinned frequency.

In order to further compare lateral stiffness of different fasteners, the change rule of wheel-rail dynamic flexibility difference rate is as shown in Figure 16(c). Based on the wheel-rail dynamic flexibility difference rate corresponding to lateral stiffness of different fasteners in Figure 16(c), when the lateral stiffness of fastener is 40 kN/mm, the wheel-rail dynamic flexibility rate is the highest, and the wheel-rail dynamic flexibility rates corresponding to the vertical stiffness of other fasteners are similar. To slow down the rail corrugation, the change of wheel-rail dynamic flexibility difference should not be too big. Through comprehensive comparison, it can be concluded that the most unfavourable value of vertical stiffness of the fastener is 40 kN/mm, and the best value range of lateral stiffness of fastener is 5–10 kN/mm.

7. Conclusions

Based on the "wheel-rail dynamic flexibility difference" mechanism, through the research on the vertical and lateral dynamic flexibility characteristics within the range of 0~1200 Hz along the longitudinal beam of the rail on different positions, this paper analyses the impact of vertical stiffness and lateral stiffness of different fasteners within half of fastener spacing on different positions along the rail at the pinned-pinned frequency on the wheel-rail dynamic flexibility difference. The following conclusion is reached.

Due to discontinuous bearing of the rail, at the pinned-pinned frequency, the dynamic flexibility of rail above the fastener and on the mid-span section varies considerably. Above

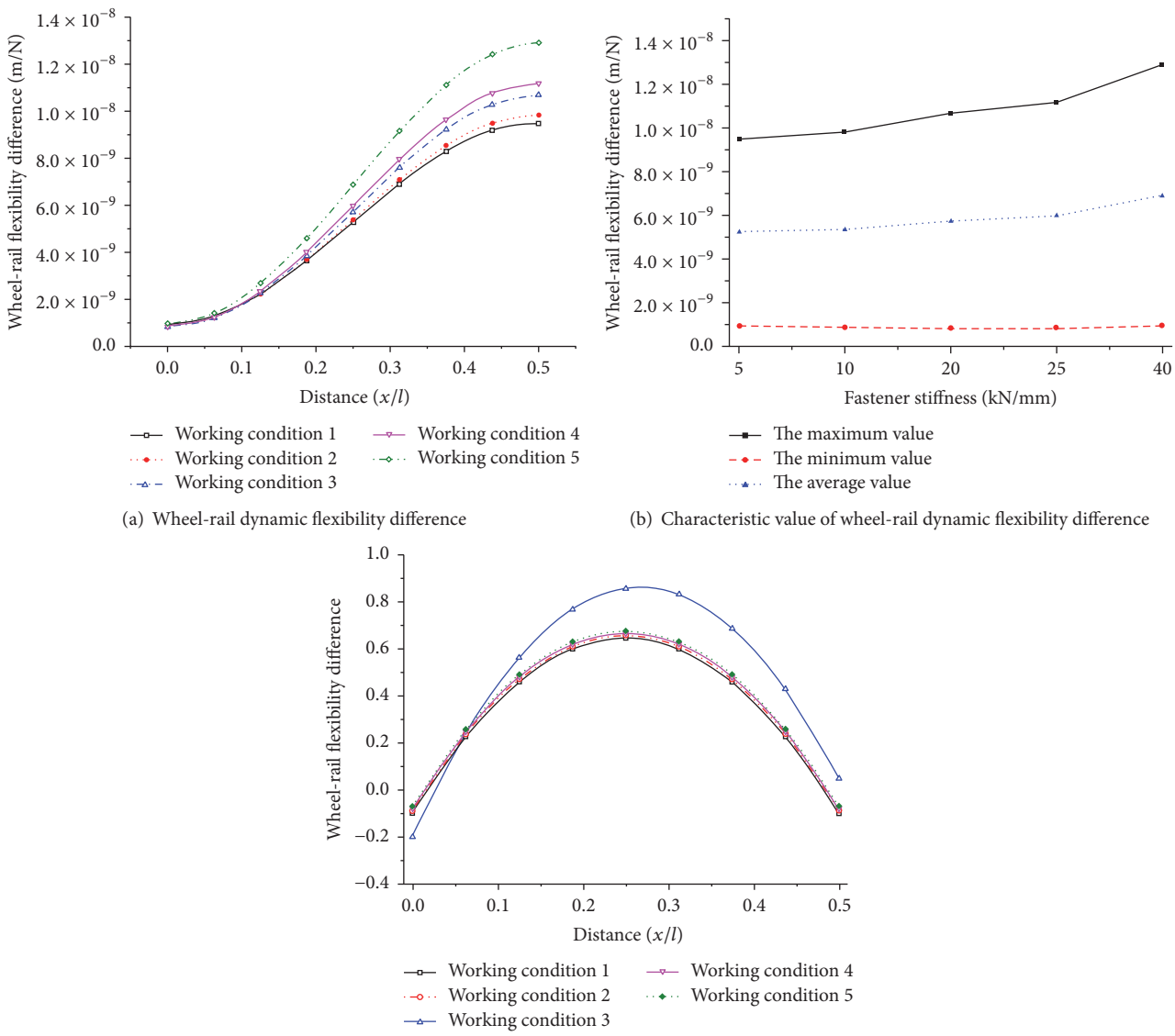

(a) Wheel-rail dynamic flexibility difference

(b) Characteristic value of wheel-rail dynamic flexibility difference

(c) Wheel-rail dynamic flexibility difference rate

Figure 15: Different vertical stiffness of fastener.

Table 3: Design of cases for the lateral stiffness of the fastener.

Fastener parameter	Case 1	Case 2	Case 3	Case 4	Case 5
Vertical stiffness/kN·mm^{-1}	40	40	40	40	40
Vertical damp/kN·s·m^{-1}	10	10	10	10	10
Lateral stiffness/kN·mm^{-1}	5	10	20	25	40
Lateral damp/kN·s·m^{-1}	10	10	10	10	10
Fastener spacing/m	0.625	0.625	0.625	0.625	0.625

the fastener its dynamic flexibility significantly decreases and the valley is presented. At mid-span its dynamic flexibility significantly increases, and the peak is presented. When the rail is at pinned-pinned frequency, the dynamic flexibility on different positions of the rail increases at first and decreases later above the fastener in the mid-span above the fastener. The change is cyclical. Such dramatic dynamic flexibility change has a great influence on rail corrugation.

At the pinned-pinned frequency, the lateral wheel-rail dynamic flexibility difference is much greater than the vertical wheel-rail dynamic flexibility difference. The short-pitch corrugation mainly appears on the curve track with large radius. It may be associated with the large lateral wheel-rail exciting force. To reduce the wheel-rail dynamic flexibility difference and rail vibration, so as to slow down and control the angle of the rail corrugation, when vertical stiffness of the

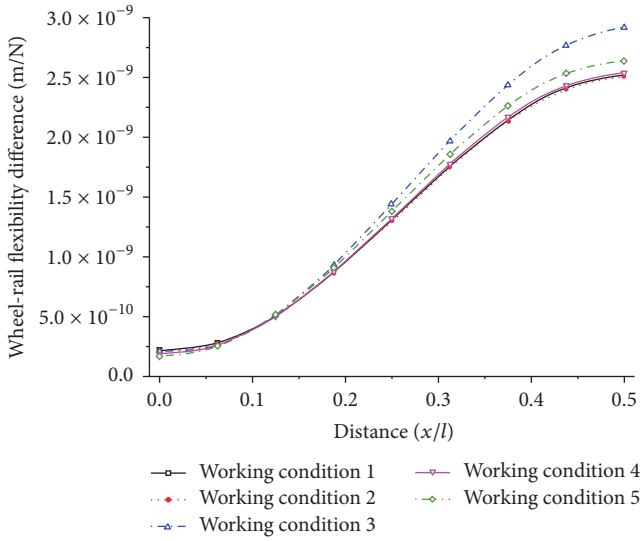

(a) Wheel-rail dynamic flexibility difference

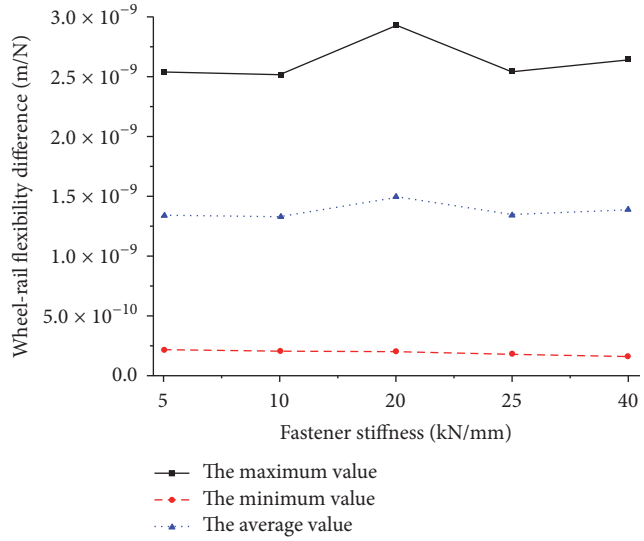

(b) Characteristic value of wheel-rail dynamic flexibility difference

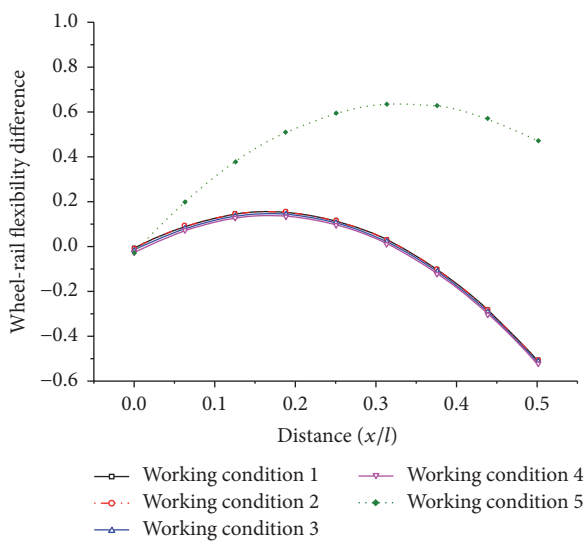

(c) Wheel-rail dynamic flexibility difference rate with lateral stiffness of different fasteners

Figure 16: Lateral stiffness of different fasteners.

fastener is 10 kN/mm, the wheel-rail dynamic flexibility difference is the minimum. When the lateral stiffness of fastener is 5 kN/mm, the wheel-rail dynamic flexibility difference is the minimum.

We should reduce the wheel-rail dynamic flexibility difference, and the wheel-rail dynamic flexibility difference rate should not be too high. The most unfavourable value of vertical stiffness of fastener is 20 kN/mm, and the best value of vertical stiffness of fastener is 10 kN/mm; the most unfavourable value of lateral stiffness of the fastener is 40 kN/mm, and the best values of lateral stiffness of the fastener are 5–10 kN/mm.

Conflicts of Interest

The authors declare that they have no conflicts of interest.

Acknowledgments

Thanks are due to the NSFC (National Natural Science Foundation of China, no. 51425804) for the research grant awarded to the corresponding author. The work described in this paper was supported by the National Natural Science Foundation of China (51508479) and the Research Fund for the Key Research and Development Projects in Sichuan Province (2017GZ0373).

References

[1] K. W. Ngai and C. F. Ng, "Structure-borne noise and vibration of concrete box structure and rail viaduct," *Journal of Sound and Vibration*, vol. 255, no. 2, pp. 281–297, 2002.

[2] H. Xia, N. Zhang, and Y. M. Cao, "Experimental study of train-induced vibrations of environments and buildings," *Journal of Sound and Vibration*, vol. 280, no. 3, pp. 1017–1029, 2005.

[3] W. Liu, W. Liu, Z. Wu et al., "Experimental study of the governance of rail corrugation of shear damper fastener in Beijing Subway," *Journal of Mechanical Engineering*, vol. 51, no. 21, pp. 73–79, 2015.

[4] Z. Liang, "Experimental study of corrugation measures for the curve track in Shanghai," *Journal of Urban Rail Transportation Research*, no. 9, pp. 62–66, 2009.

[5] Y. Yan, "Analysis on corrugation of curve rail with small radius of Guangzhou Metro Line 5," *Research on Urban Mass Transit*, no. 6, pp. 55–57, 2011.

[6] S.-L. Lian, Q. Sun, and W. Wang, *Railway Curve Rail Corrugation and Its Mitigation Measures*, China Railway Publishing House, Beijing, China, 2001.

[7] X. Lei and X. Sheng, *Noise and Vibration of Railway Traffic*, Science Press, Beijing, China, 2004.

[8] J. T. Neslson, "Wheel-rail noise control manual".

[9] P. J. Remington, "Wheel/rail noise—part IV: rolling noise," *Journal of Sound and Vibration*, vol. 46, no. 3, pp. 419–436, 1976.

[10] B. Hemsworth, "Recent developments in wheel/rail noise research," *Journal of Sound and Vibration*, vol. 66, no. 3, pp. 297–310, 1979.

[11] Y. Sato, A. Matsumoto, and K. Knothe, "Review on rail corrugation studies," *Wear*, vol. 253, no. 1-2, pp. 130–139, 2002.

[12] S. L. Grassie and J. Kalousek, "Rail corrugation: characteristics, causes and treatments," *Proceedings of the Institution of Mechanical Engineers, Part F: Journal of Rail and Rapid Transit*, vol. 207, no. 1, pp. 57–68, 1993.

[13] Vailivia, "The Interaction between high-frequency wheel-rail dynamics and irregular rail wear-a linear model," VDI Fortschritt-Berichte, 12–93, VDI-Verlag Düsseldorf, 1988.

[14] S. L. Grassie, "Rail corrugation: characteristics, causes, and treatments," *Proceedings of the Institution of Mechanical Engineers, Part F: Journal of Rail and Rapid Transit*, vol. 223, no. 6, pp. 581–596, 2009.

[15] X. Lei, "Rail grinding principle and its application," *Journal of Railway Engineering*, no. 1, pp. 28–33, 2000.

[16] R. Heyder and G. Girsch, "Testing of HSH® rails in high-speed tracks to minimise rail damage," *Wear*, vol. 258, no. 7-8, pp. 1014–1021, 2005.

[17] M. Tomeoka, N. Kabe, M. Tanimoto, E. Miyauchi, and M. Nakata, "Friction control between wheel and rail by means of on-board lubrication," *Wear*, vol. 253, no. 1-2, pp. 124–129, 2002.

[18] J. I. Egana, J. Vinolas, and M. Seco, "Investigation of the influence of rail pad stiffness on rail corrugation on a transit system," *Wear*, vol. 261, no. 2, pp. 216–224, 2006.

[19] T. X. Wu, "Effects on short pitch rail corrugation growth of a rail vibration absorber/damper," *Wear*, vol. 271, no. 1-2, pp. 339–348, 2011.

[20] Z. Wen, *Study on rail corrugation [Ph.D. thesis]*, Southwest Jiao Tong University, 2006.

[21] A. B. Wang, Z. Q. Wang, P. Zhang, N. Xu, Z. Zhang, and K. He, "Study on the mechanism of discontinuous support stiffness on the development of rail corrugation," in *Proceedings of the 21st International Congress on Sound and Vibration (ICSV '14)*, pp. 1926–1933, Beijing, China, July 2014.

[22] K. Hempelmann, *Short-Pitch Corrugation on Railway Rails: A Linear Model for Prediction*, VDI Fortschritt-Berichte 12-231, VDI-Verlag, Düsseldorf, Germany, 1994.

[23] K. Knothe and B. Ripke, "The effects of parameters of wheelset, track and running conditions on the growth rate of rail corrugation," *VSD (Supplement)*, vol. 18, pp. 345–356, 1989.

[24] A. Gu, W. Liu, H. Zhang, and X. Sun, "The impact of subway fastener stiffness and damp on the abnormal rail corrugation," *Urban Rapid Rail Transit*, vol. 24, no. 3, pp. 17–21, 2011.

[25] A. Wang, Z. Wang, Z. Zhao et al., "Effects of track stiffness and tuned rail damper on rail roughness growth and rail vibration levels on metro systems," in *Proceedings of the 11th International Workshop on Railway Noise*, Uddevalla, Sweden, 2013.

[26] L. Liu, Y. Xuan, and J. Sun, "Study on solving the rail admittance based on Timoshenko beam," *Railway Construction*, no. 5, pp. 136–138, 2012.

[27] Y. Han, "Analysis on the vibration and noise reduction and the engineering measures of urban rail transit," *Journal of Railway Engineering*, vol. 2, pp. 85–88, 2010.